ELECTROLYSIS OF $TbCl_3$ AND $DyCl_3$ TO PRODUCE RARE EARTH-IRON MASTERALLOYS USING A CONSUMABLE IRON CATHODE

Johan Sundström

Department of Metallurgy, The Royal Institute of Technology, S-100 44 Stockholm.

Present address: Swedish Institute for Metals Research, Drottning Kristinas väg 48, S-114 28 Stockholm. (johan.sundstrom@simr.se)

Keywords: rare earth metal, terbium, dysprosium, molten salt, electrolysis, current efficiency

ABSTRACT

Preparation of rare earth-iron alloys was conducted by electrolysis of a molten RCl_3-AX salt (R=Tb and Dy, A=K or Li, X=Cl or $Cl_{0.5}F_{0.5}$) using a consumable iron cathode. Optimum conditions with respect to cathode current efficiency (CCE) was obtained in the compositional range 15-20 mol% RCl_3. CCE was low; in general not exceeding 10% for $DyCl_3$ electrolysis and 30% for $TbCl_3$ electrolysis. CCE increased with cathode current density (CCD) up to the maximum values set by the occurrence of limiting currents (CCD_{lim}), which was a phenomena characterized by an irreversible increase of the electrical resistance. Oxidation of the electrolyte was occurring as evidenced by sludge formation. The role of rare earth dichloride (subchlorides), formed at the cathode, is discussed in terms of CCE and sludge formation (oxidation). Means to improve the conditions for electrolysis with respect to productivity and oxygen content in the recovered alloy are discussed.

1 INTRODUCTION

Tb- and Dy metals are important constituents in "Terfenol-D"^{TM}, which is an intermetallic compound ($Tb_{0.27}Dy_{0.73}Fe_2$) used for its giant magnetostrictive properties in materials for sensors and active vibration; high-power transducers, electric actuators and motors; and geophysical exploration tools. Another use of Tb metal is in amorphous $TbFe_2$ used in magneto-optic storage devices for data process technology and computer systems. The success of these materials is dependent upon the cost of producing the rare earth metals/alloys, which often must fulfill stringent quality specifications with regard to impurity elements. One of the most harmful elements is oxygen, which if permitted dissolves up to some few atomic percents in the rare earth metals. The problem of oxygen with regard to the preparation and properties of rare earth intermetallic compounds has been discussed by Gschneidner & Ellis [1-4]. Thus, in order to develop a suitable process for rare earth metals production, an important criterion is to obtain metals of low oxygen content.

Metallothermic processes for Tb and Dy are based on fluorides as precursor compounds, which are reduced with calcium at elevated temperatures in order to obtain a molten metal/alloy pool. This is a batch-wise process, which needs a subsequent vacuum treatment in order to remove dissolved calcium. Oxygen may follow in large amounts from calcium and the fluoride precursor compound if not special purification measures are made in advance. On the other hand, electrochemical reduction processes do not require the use of expensive reducing agents and offer the possibility of continuous operation.

Morrice [5] has reviewed the electrolytic production of rare earth metals. Due to the much lower electrode potentials of rare earth metals compared to hydrogen, aqueous electrolytes are not possible to use. Therefore, processes for the electrolytic recovery of rare earth metals are confined to molten salt electrolytes. Fluorides, oxyfluorides and chlorides of rare earths mixed with alkaline- and alkaline earth-halides have been used. Pure rare earth fluorides are not commonly adopted as electrolytes, because they are expensive and form deleterious carbonfluorides at the graphite anode. Oxyfluoride electrolytes have the advantage of making use of the less costly rare earth oxides to feeding the cell. But because of low oxide solubility, significant amounts of carbonfluorides may evolve from the anode here as well and the "anode effect", which is

characterized by an irreversible increase in the electrical resistance by a carbonfluoride gas layer at the anode, is difficult to avoid [6].

Comparatively, chloride electrolytes can be electrolyzed in a smoother operation and with less corrosion on cell materials. The most frequently used arguments against using rare earth chlorides have been their hygroscopic properties and cumbersome dehydration procedures. However, by the development of a novel process based on fluidized bed dehydration [7], pure and anhydrous rare earth chlorides are made possible for recovery at a low cost and high productivity. With the exclusion of crystallized water and oxide impurities from the rare earth chlorides, electrolysis by the chloride route appears to possess an inherent advantage over oxyfluoride electrolysis in its potential to produce metals of low oxygen content. But in order to realize this, a decisive issue is to control the extent of electrolyte oxidation by atmospheric oxygen and moisture during electrolysis.

The high solubility of rare earth metals in their molten trichlorides appears to be the main disadvantage of using them as electrolytes. This phenomena is responsible to the low cathode current efficiency (CCE) and thereby low productivity, experienced in both lab-scale electrolysis and industrial electrolysis [8,9]. The term solubility may be misleading, since it is rather a question of valence instability between the tripositive and dipositive state, which results in the reaction:

$$R_{(\text{in metal phase})} + 2RCl_{3(\text{in salt phase})} \rightarrow 3RCl_{2(\text{in salt phase})} \quad (1)$$

Much work in this area of research was conducted by Corbett & associated and is well summarized in [10]. As can be seen in Figure 1, the equilibrium of reaction 1 varies considerably between the different rare earth elements. Based on these data, it may be predicted that $DyCl_3$ electrolysis is unfavorable with regard to CCE; correspondingly, $TbCl_3$ electrolysis is predicted to yield better results. However, the final productivity of rare earth chloride electrolysis is much dependent of other factors, such as cell design, electrolyte composition and temperature. In principal, excessively high temperatures are detrimental due to the increasing loss of rare earth chlorides by vaporization and an increasing equilibrium constant of reaction 1. For practical purposes, the cell temperature should be higher than the melting point of the metal/alloy formed

at the cathode. Due to the high melting points of Tb- and Dy metal, it is not possible to produce them non-alloyed by chloride electrolysis. A low melting R-Fe eutectic alloy (80-90 w% R, T_m<1000°C) could be formed by the use of a consumable iron cathode. The production of terbium- and dysprosium-iron masteralloys instead of their pure metals is justified by the fact that iron constitutes a major part in the intermetallic end product.

The following work was conducted with the aim of finding out the feasibility of chloride electrolysis to produce Tb-Fe and Dy-Fe masteralloys. Another aim is to identify critical parameters of rare earth chloride electrolysis in general, which may be addressed to the preparation of other more commercially important rare earth metals/alloys. Special attention has been devoted to the cathode current efficiency (CCE). CCE is a decisive measure of the economical viability of electrolysis, since it constitutes an important parameter for the energy consumption and productivity of the process. Terbium and dysprosium are expensive metals with market prices ranging between US$ 625-1200 and US$ 80-300 per kg, respectively, depending on purity [11]. But because of the low volumes demanded only small cells could be effectively used. This leads to a comparatively high operating cost of electrolysis. Therefore, CCE should be regarded primarily as a parameter of relevance for the productivity.

2 EXPERIMENTAL

2.1 Materials

Tb_4O_7 of 99.9% and Dy_2O_3 of 99% purity were supplied by Rhône Poulenc Chimie, France. The complete procedure to obtain $RCl_3 \cdot 6H_2O$ followed by fluidized bed dehydration to anhydrous RCl_3 is described elsewhere [7]. The purities of the finally charged rare earth chlorides varied both with respect to crystallized water content and the presence of hydrolytic compounds. In cases when hydrolytic compounds were absent or present in negligibly small amounts (indicated by the clearness of water-solutions), the content of remaining water could be determined analytically by chlorine analysis. In other cases, the content of hydrolytic compounds (arbitrarily defined as ROCl) was determined by chlorine analysis and acid-base titration; the crystallized water content was estimated from the total time of dehydration and the dehydration kinetics of the last traces

of water. LiF, LiCl and KCl were of "Pro analysi"-grade and vacuum treated at 300°C before use. Argon "Plus" of 99.996% purity (<5ppm H_2O and <5ppm O_2) and helium of 97% were supplied by AGA Gas AB, Sweden. High quality graphite was supplied by Svensk Specialgrafit AB. Pure iron (30 ppm carbon) for cathodes was supplied by Armco GmbH, Germany.

2.2 Equipment

The frame of the electrolytic cell was unchanged through all experiments and is pictured in Figure 2. Heat was supplied by a 5½ kW Kanthal furnace: "Fibrothal RAC 200/500" (h=520 mm, ID=200 mm). A closed cell atmosphere was obtained by positioning the alumina lid on the steel pot (h=480 mm, OD=168 mm and 4.5 mm thick walls). Corrosion of the steel pot on the outside by air oxidation was more rapid than inside corrosion by the Ar/Cl_2 atmosphere. To ensure gas tightness of the steel pot, a new one was taken into use after every second investigation. The alumina lid was fitted with mullite tubes for inlet and outlet gas, electrical leads and thermocouple protection tube. The center tube (ID=40 mm) served as a port for the cathode-crucible assembly as well as for feeding and sampling in the periods of cathode exchange. Graphite sleeves were used around the electrical leads in order to minimize the amount of outlet gas passing through other locations than the outlet tube.

Cell arrangement

In the first two preliminary investigations the anode was a separate graphite tube which was concentrically positioned above the cathode with its lower end in level with the cathode (see Figure 8). However, it was experienced that a proper concentric position was difficult to realize. Therefore, in the subsequent investigations a simpler cell arrangement was adopted (see Figure 2). The graphite container (h=350 mm, OD=140 mm) had the interior machined into a lower and upper compartment. The lower compartment (h=80 mm, ID=70 mm) enabled the use of small salt volumes from start. Iron cathodes were machined to identical dimensions (h=25.0 mm, D=10.0 mm) and the cathodic leads were protected by silica glass tubes. The alloy from each cathode was collected in a small Al_2O_3 crucible (5 cm^3) attached below the iron cathode. This cathode-crucible assembly was constructed by drilling a small hole through the bottom of the Al_2O_3 crucible and through the bottom of the cathode up to the screw hole for the cathodic steel lead. A tantalum

wire (D=1 mm) was threaded through both holes and both ends were squeezed in order to lodge their positions below the Al_2O_3 crucible and in the cathode, respectively. To further strengthen a stable position of the hanging crucible, a small amount of refractory cement was applied below the bottom hole of the crucible. The thermocouple protection tube was fitted into a drilled hole at the rim of the lower compartment.

2.3 Procedure

Before use, the cathodes were surface cleaned by washing first in dilute hydrochloric acid, then in distilled water followed by 99% ethanol and finally quickly dried by blowing hot air. Investigations were started by flushing argon into the closed cell for at least one hour. The initial salt mixture was then charged through the feeding port. While argon was flowing constantly at 6 l/min, the cell was heated up to the desired temperature of electrolysis. The feeding port was plugged by a rubber stopper during this treatment. After the cathode-crucible assembly had been submerged into the molten salt, current was slowly increased up to the desired value. Current was held constant by automatic regulation and the cell voltage was continuously recorded. After the desired time of electrolysis the cell power was switched off and the cathode-crucible assembly was gently withdrawn from the cell. Then it was quickly submerged into a vertical tube and flushed by helium from below for cooling. The Al_2O_3-crucible was broken and the alloy recovered for subsequent weighing and analysis. A new cathode-crucible assembly was then submerged and the procedure was repeated until the total number (15-25) of cathodes were electrolyzed in each investigation.

2.4 Analysis

X-ray Fluoroscence Spectrometer (XRF). Individual rare earth elements and potassium in salt samples were analyzed as dissolved elements in water solutions against calibrated data and standard solutions. Alloy samples were first dissolved in nitric acid, then boiled to a dry nitrate powder which was heat treated at 1000°C in at least 24 hours to finally obtain a finely ground oxide. This powder was then melted with lithiumborate flux to glassy homogeneous buttons for analyse against calibrated data and standard samples.

Complexometric titration with Titriplex® (E. Merck, Darmstadt, Germany) of total rare earth content in salt samples. This method was used after chlorine had been removed from the solution by AgCl-precipitation and filtration.

Silver chloride gravimetry for chlorine analysis.

Acid-base titration for determination of oxide content in chloride salts.

Carbon and oxygen in alloy were analyzed with LECO instruments.

3 RESULTS

The present results are based on seven investigations, totally electrolyzing a number of 125 cathodes each at a period of time usually within 30-60 minutes. In five of seven investigations, the experimental conditions were varied more or less in an arbitrary manner and therefore details have been omitted in the following paper. However, some important observations were made leading to conclusions, which in the following section, are reported to have been derived from the "preliminary investigations". Because of comparative experimental conditions the other two investigations on $DyCl_3$- and $TbCl_3$ electrolysis are reported more in detail in Section 3.2.

3.1 Preliminary investigations

The preliminary investigations were electrolyzing $(Tb_{0.27}Dy_{0.73})Cl_3$ and $DyCl_3$ in various alkali halide mixtures: KCl; LiCl; and equimolar LiCl/LiF. The first two investigations were carried out without fluoride addition and with the cell arrangement slightly different from that shown in Figure 2. Here, a separate graphite tube was adopted as anode and placed in a concentric position above the cathode with its lower end in level with the cathode (see also description in Section 2.2). Analytical results from molten salt samples taken frequently throughout these investigations showed that the bulk of electrolyte was consistently pure with respect to oxide-contamination and preserved in its rare earth trichloride ground state (samples dissolved in clear light-yellow solutions with water). Exception being the black salt inside the alloy-collecting crucible, which

was considerably reduced with a composition closely corresponding to a rare earth dichloride. In the three following investigations the graphite container served as anode according to Figure 2 and a LiCl/LiF-base electrolyte was used. This type of electrolyte improved results in terms of CCE, a finding that supports the beneficial effect of fluoride additions as have been stated by Seon [12]. On the other hand, it was experienced that these investigations were related with a detrimental accumulation of sludge in the electrolyte. Analyses disclosed it to be virtually chlorine-free, with a few percents carbon and with rare earth and fluorine contents approximately corresponding to a rare earth oxyfluoride.

Temperature variations within the limited interval 920-1000°C had a small influence on the resulting yields in terms of CCE. Another parameter of relative insignificance was carbon content in iron cathodes, which did not show any decisive effect on CCE within the studied interval: (<10)-1000 ppm. This observation is contradicting the reported large effect of carbon on CCE in $NdCl_3$ electrolysis [13]. On the other hand, a clear relationship was obtained between CCE and RCl_3-concentration in the studied interval 10-70 mol%; best results were obtained at concentrations between 15 and 20 mol% RCl_3 in the electrolyte. Although it was hypothesized that a composition corresponding to the stable compound K_3RCl_6 [14] would stabilize the R^{3+} ion in the electrolyte and thus increase the yields in terms of CCE, results at the equivalent composition of 25 mol% RCl_3 showed the opposite result.

Cathode current density (CCD) was a parameter of fundamental importance for the results in terms of CCE. At CCD up to about 3-5 A/cm^2 CCE was practically zero. At higher values, CCE was increasing with CCD, but only up to the occurrence of limiting currents (CCD_{lim}) from which the current could not be exceeded. This phenomenon was characterized by an irreversible voltage rise together with a current fall, indicating some sudden increase in the electrical resistance. Satisfactory conditions were only re-established by switching off the power for some minutes and then very slowly increasing the current again. By decreasing the interelectrode distance CCD_{lim} was increased, but without increasing the maximum achievable CCE.

3.2 Final investigations

Electrolysis of $TbCl_3$

1748 g $TbCl_3$, containing 0.98 mol% TbOCl and less than 1 mol% H_2O, was charged together with 901 g LiCl/LiF equimolar mixture, thus making up a composition of 20 mol% $TbCl_3$. 25 cathodes were electrolyzed and the experimental data and results of these are reported in Table 1. Totally 342.3 grams of Tb-Fe alloy was recovered. Based on the concentration of Tb in the alloy, the end concentration of $TbCl_3$ in the electrolyte was estimated to be 15 mol%.

Because of the relatively high degree of cathode consumption in these experiments, CCD was calculated based on the linearly averaged area of the cathode before and after electrolyzed. In C16 the crucible (with alloy) was lost to the bottom of the cell during the cathode was collected. Since the graphite cell was anodized, it might be expected that the alloy poured out from the crucible to become anodically redissolved from then. However, the alloy yield calculated from the cathode consumption was found to be remarkably high at the high CCD used. In C20 the cathode and crucible were covered by sludge and the yield was considerably lower. Sludge was present in the electrolyte also during the last following cathodes C21-C25, but in comparison with $DyCl_3$ electrolysis the amount of sludge was less. From C20, CCD_{lim} had decreased from a high level (>20-25 A/cm^2) down to a level between 12-15 A/cm^2, which apparently occurred in conjunction with sludge formation.

Alloy from cathode C2 was containing 1280 at-ppm oxygen and 490 at-ppm carbon. Figure 3 illustrates the analyzed Tb-content of all alloys plotted against the temperature of electrolysis, which shows that the recovered alloys were completely liquidus during electrolysis (68-77 at% Tb).

Electrolysis of $DyCl_3$

1500 g $DyCl_3$, containing 0.42 mol% DyOCl and less than 1 mol% H_2O, was charged together with 760 g LiCl/LiF equimolar mixture, making up a composition of 20 mol% $DyCl_3$. 16 cathodes were electrolyzed. Pertinent experimental data and results are reported in Table 2. Based on the total amount of recovered Dy in alloy, the end concentration of $DyCl_3$ was estimated to 18 mol%.

With time, sludge of a dysprosium oxyfluoride type was accumulating to the molten salt surface and in the bottom of the graphite crucible. In frequent cases sludge was found around and below the cathode. The magnitude of limiting currents was in the same range as in the preliminary investigations, i.e. at 10-12 A/cm^2.

Alloy from cathode C2 was analyzed to contain 2220 at-ppm oxygen and 1300 at-ppm carbon. Figure 4 illustrates the analyzed Dy-content of all alloys plotted against the temperature of electrolysis (=950°C). As can be seen the compositions (66-70 at% Dy) are in close vicinity around the liquidus line, which implies the presence of solid $DyFe_2$-phase during electrolysis in some of the recovered alloys. This matter has been evidenced by microstructural investigations. Figure 5 shows the microstructure of the former liquid film around the cathode.

4 DISCUSSION

Comparison between $TbCl_3$- and $DyCl_3$ electrolysis

As has been mentioned in the introduction, CCE is a decisive parameter for the process and in first hand of relevance to the productivity in preparing the expensive alloys of Tb-Fe and Dy-Fe. Figure 6 shows CCE plotted versus CCD for $TbCl_3$- and $DyCl_3$ electrolysis from the final investigations. The low CCE of $DyCl_3$ electrolysis suggests that this process is unsuitable to adopt for Dy-Fe alloy production. On the other hand, $TbCl_3$ electrolysis results in twice as high CCE at the same CCD and allows for electrolysis at a comparatively higher CCD. Considering the fact that Tb metal is more expensive than Dy metal, it may be suggested that $TbCl_3$ electrolysis has a potential to become economically viable for Tb-Fe alloy production. The relatively low carbon- (490 at-ppm) and oxygen (1280 at-ppm) content of obtained Tb-Fe alloy give additional support to this conclusion.

The reported cell voltage of cathode C17 in Table 1 is abnormally low, as it is lower than theoretically possible for $TbCl_3$ electrolysis (~2.6 V). The reported cell voltage of cathodes C18 and C19 are unusually low as well. A possible reason is related to the redissolution of the

unrecovered alloy from cathode C16, which effectively reduced cell voltage, by direct anodic oxidation of the lost alloy or/and anodic oxidation of Tb^{2+} that formed in excessive amounts according to reaction 1.

Oxygen content in alloy

Although the analyzed oxychloride content in the feed material was more than twice as high in $TbCl_3$ compared to $DyCl_3$, the final oxygen content in the Tb-Fe alloy was almost half of the content in the Dy-Fe alloy. This indicates that kinetic factors are important to the final oxygen content of alloy, which means that the rate of alloy formation compete with the rate of oxygen entering into the alloy from the electrolyte. If oxy-anions in the electrolyte are chemically bound to trivalent rare earth cations in the form of rare earth oxychlorides, the transfer of oxygen might be realized by the following reaction:

$$(2+x)ROCl_{\text{(in salt)}} = (1+x)R_{\text{(in alloy)}} + (2+x)O_{\text{(in alloy)}} + xRCl_{3\text{ (in salt)}} + (1-x)RCl_{2\text{ (in salt)}} \quad (2)$$

The rate of reaction 2 is probably diffusion limited with regard to the transport of ROCl to the alloy surface. Accordingly, high alloy productivity and a low oxy-anion content in the molten salt are the beneficial factors for low oxygen content in rare earth alloys. The significance of the latter factor was later on demonstrated by deliberately feeding $DyCl_3 \cdot H_2O$ for a LiCl-based electrolyte. The effect on alloy quality was clearly visible by the fresh-cut surfaces exhibiting a grayish color without the metallic luster of previous samples. The oxygen content was 15 300 at-ppm (1.53 at%), which is almost a factor ten higher than the corresponding composition using an anhydrous feed.

Sludge

Sludge, which occurred in all investigations except in the first two preliminary investigations, seems to be a critical problem on a long-term basis. Results from $TbCl_3$ electrolysis indicated that sludge formation and decreasing limiting currents (CCD_{lim}) are interrelated phenomena. Sludge could clad to the cathode surface and disturb alloy formation and dripping off cathode, effectively decreasing CCE. If sludge accumulates to the molten bath, it has to be removed by some means;

which may render the realization of a closed cell performance more difficult. Analytical results showed that sludge in a LiCl/LiF base electrolyte was of a rare earth oxyfluoride type, which give reasons to believe that fluoride additions decrease the solubility of sludge in molten salts. Comparing the remarkably high solubility of Nd_2O_3 in $NdCl_3$ [16] shown in Figure 7, with its corresponding solubility in NdF_3, reported to be some few weight percents [17], also supports this hypothesis.

However, the basic reason to sludge formation is supersaturating preceded by an accumulating amount of dissolved oxy-anions in the molten salt. Since the cell was incompletely closed and frequent openings of the cathodic port were made during the investigations, significant amounts of oxygen may have leaked into the cell atmosphere. Thus, small but not insignificant oxygen potential is assumed to have prevailed over the molten bath through all investigations. Having this background in mind, the purity of electrolyte and absence of sludge experienced for the first two preliminary investigations are anomalies which might be explained if the mechanism of oxidation could be unravelled.

Mechanism of electrolyte oxidation

Table 3 lists the conceivable reactions responsible for atmospheric oxidation together with their equilibrium constants at 900°C. R=Nd has been chosen as a comparison because more thermodynamic data are available for compounds NdOCl [18] and $NdCl_2$, and the stabilities of $NdCl_2$ and $DyCl_2$ are comparatively equal (see Figure 1). The formation enthalpy of $NdCl_2$ was measured by Morss and McCue [19] to -706.9 kJ/mol and entropy estimated by Latimer's rule [20] to 126 J/mol·K. Finally the heat capacity data of $SmCl_2$ [18] were adopted. In view of the values in Table 3, oxidation of the melt may be kept fairly limited, at reasonably low oxygen potentials over the melt, as long as the trichloride state is concerned. The chlorine potential that is established by evolving chlorine gas during electrolysis further helps to suppress the O_2-oxidation reaction. On the other hand, data on oxidation of $NdCl_2$ implies unlimited reactions in the sense that even the smallest traces of oxygen in the cell atmosphere are capable to react. Because of the low yields in terms of CCE, a large proportion of the consumed current was apparently wasted for the formation of rare earth dichlorides. The constant supply of RCl_2 from the cathode to the bulk of electrolyte may therefore serve for reactions 5 and 6 (Table 3) to take

place, provided that a partial flow of RCl_2 is permitted to reach the surface of the molten bath before being anodically oxidized back to RCl_3. The proposed mechanism is thereby relating low CCE, with a corresponding high concentration of dichlorides, with high susceptibility for atmospheric oxidation (as might be experienced by excessive amounts of sludge). This is in accordance with the results reported in Section 3.2.

By comparing the cell arrangement used in the two first preliminary investigations (see Figure 8) with the cell arrangement used in the subsequent investigations (Figure 2), the occurrence of oxidation and sludge in the latter may be attributed to the mechanism proposed above. The cell arrangement illustrated in Figure 2 makes it possible for a large proportion of the RCl_2-rich catholyte flow to reach the molten bath surface. On the other hand, the use of a separate anode tube hanging concentrically above the cathode as illustrated in Figure 8, appears to effectively shield off this flow by anodically oxidizing RCl_2 back to RCl_3 before entering the surface of the molten bath.

Limiting currents and productivity

An important issue to solve in future work is the reason for limiting currents and how CCD_{lim} can be increased in order to permit higher CCD. According to Figure 6, there seems to be scope to increase CCE by increasing CCD, which thereby would multiply to the total effect on productivity defined as:

$$Productivity = \frac{CCD \cdot CCE \cdot M_R}{100 \cdot 3F} \quad (7)$$

M_R represents the molar weight of the specific rare earth element and F represents Faraday's number. Productivity is here expressed with the unit: $g/(cm^2 \cdot s)$, where the area unit refers to the working area of the cathode.

In the case of $DyCl_3$ electrolysis, limiting currents started to occur above 10-12 A/cm^2 for an interelectrode distance of about 3 cm. In the case of $TbCl_3$ electrolysis, CCD_{lim} was above 20-25 A/cm^2 during the first 17 cathodes. However, after sludge first appeared in C20, CCD_{lim} was reduced to a level in the range of 12-15 A/cm^2. Thus, the phenomena of limiting currents could be related to the formation of sludge. Bjørgum et al. [21] found a similar phenomena of limiting

currents occurring in the electrolysis of $AlCl_3$, which they ascribed to be a result of cathodic passivation by precipitation of aluminium oxide. A corresponding mechanism based on rare earth oxide or oxyfluoride precipitation could serve to explain the limiting currents in the present work.

5 CONCLUSIONS

Preparation of R-Fe alloys (R=Tb, Dy) was conducted by electrolysis of a molten RCl_3-AX salt (A=K or Li; X=Cl or $Cl_{0.5}F_{0.5}$) using a consumable iron cathode. Optimum conditions with respect to cathode current efficiency (CCE) was obtained in the compositional range 15-20 mol% RCl_3. CCE was low; in general, not exceeding 30% for $TbCl_3$ electrolysis and 10% for $DyCl_3$ electrolysis. The main reason to low CCE is due to the formation of RCl_2 at the cathode, which is subsequently reoxidized to RCl_3 at the anode following a cyclic behavior during electrolysis. The stability of RCl_2 as compared between R=Tb and R=Dy, reflects the different yields in terms of CCE. CCE increased with cathode current density (CCD) up to the maximum values set by the occurrence of limiting currents (CCD_{lim}), which was a phenomena characterized by an irreversible increase of the electrical resistance. Passivation of the cathode surface by precipitation of rare earth oxide- or oxyfluoride compound was proposed as a possible reason to limiting currents. Based on productivity, Tb-Fe alloy production by $TbCl_3$ electrolysis appears promising as an economically viable process. In general, further scope to increase productivity will be obtained if CCD_{lim} can be increased. The composition of alloys was in the range of 66-70 at% Dy and 68-77 at% Tb, respectively. Oxygen content was 2220 at-ppm in a Dy-Fe alloy and 1280 at-ppm in a Tb-Fe alloy.

In order to secure a stable process on a long-term basis, excessive sludge formation must be avoided. Adding fluorides to the molten chloride salt appears to decrease the solubility of sludge as a consequence of rare earth oxyfluoride sludge formation. However, fluorides improve the productivity of electrolysis with respect to CCE. Therefore, the most effective approach towards a sludge free electrolyte is to avoid oxidation from atmosphere. Thermodynamic calculations have shown that the presence of rare earth dichlorides at the molten salt surface promotes oxidation. Thus, apart from adopting a closed cell performance, an important feature of the cell design must

consider the RCl_2-rich catholyte flow with the purpose to shield off this flow by the anode and establish complete anodic conditions (RCl_3) at the molten bath surface.

ACKNOWLEDGEMENTS

This work has been carried out with the financial support from NUTEK (The Swedish Board for Industrial and Technical Development) which is gratefully acknowledged. The author is also indebted to thank Mr. Brant Zell at the Rhône-Poulenc Inc./Phoenix Plant for conducted analyses on elemental carbon and oxygen.

SYMBOLS

CCD	cathode current density	A/cm^2
CCE	cathode current efficiency	%
D	diameter	m
F	Faraday's number	A·s/mol
h	height	m
I	current	A
ID	inside diameter	m
K	constant	-
M	molar weight	g/mol
m	mass	g
OD	outside diameter	m
R	rare earth element (arbitrary)	-
T	temperature	°C
t	time	min
U	cell voltage	V

SUBSCRIPTS

a	alloy
av	average
eq	equilibrium
i	initial
lim	limited
m	melting

REFERENCES

[1] "Preparation and Purification of Rare Earth Metals and Effect of Impurities on Their Properties", Gschneidner, K.A. Jr., in **Science and Technology of Rare Earth Materials**, Academic Press Inc., 1980.

[2] "Metals, alloys and compounds - high purities do make a difference!", Gschneidner, K.A. Jr., **Journal of Alloys and Compounds**, Vol. 193 (1993), 1-6.

[3] "Pure Rare Earth Metals for Today's and Tomorrow's Advanced Technologies", Gschneidner, K.A. Jr. and Ellis, T.W., in **Metallurgical Processes for Early Twenty-First Century**, ed. H.Y. Sohn, TMS Annual Meeting, San Diego, California, 1994.

[4] "Effects of Oxygen on the Solidification Microstructure of $LaNi_5$", Ellis, T.W., Jones, L.L., and Bloomer, T.E., **Journal of Metals**, Feb. 1995, 47-49.

[5] "Fused-Salt Electrowinning and Electrorefining of Rare-Earth and Yttrium Metals", Morrice E. and Wong M.M., **Minerals Science Engineering**, Vol. 11, No. 3 (1979), 125-136.

[6] "Anode Effect in Neodymium Oxide Electrolysis", Keller, R. and Larimer K.T., in **Rare Earths - Science, Technology & Applications**, eds. Bautista R.G., Bounds C.O., Ellis T.W. and Kilbourn B.T., TMS Annual Meeting, Orlando, Florida, 1997.

[7] "Preparation of $DyCl_3$ by Dehydration in a Fluidized Bed", Sundström J., in **Rare Earths - Science, Technology & Applications**, eds. Bautista R.G., Bounds C.O., Ellis T.W. and Kilbourn B.T., TMS Annual Meeting, Orlando, Florida, 1997. (Supplement 4)

[8] "Relationship Between the Dissolution Behaviours and Current Efficiencies of La, Ce, Pr and Nd in Their Chloride Molten Salts", Feng L., Guo C., and Tang D., **Journal of Alloys and Compounds**, Vol. 234 (1996), 183-186.

[9] "Investigation on Current Efficiency in the Electrolysis of Molten $RECl_3$-KCl Salt", Liu Y., **Journal of the Chinese Rare Earth Society**, Vol. 4, No. 2 (1986), 61-65. (In Chinese)

[10] "Reduced Halides of the Rare Earth Elements", Corbett J.D., **Revue de Chimie minérale**, Vol. 10 (1973), 239-256.
[11] A compilation of Market Prices in **ELEMENTS - Rare Earths, Specialty Metals and Applied Technology** (a Trade Tech Publication), Vol. 6, No. 1 (1997), 4.
[12] "Preparation of Neodymium-Iron Master Alloys from Neodymium (III) Salts and Metallic Iron in Molten Chloride-Fluoride Mixtures", Seon F.M., Proceedings of the Joint Inter-national Symposium on Molten Salts, **Electrochemical Society**, Vol. 87 (1987), 835-845.
[13] "Consumable Cathode Selection in the Production of Neodymium-Iron Alloys Via Molten Salt Electrolysis", Earlam M.R., **Metallurgical Transactions B**, Vol. 21B (1990), 599-600.
[14] "Phase Diagram of Ternary $DyCl_3$-KCl-NaCl System", Mochinaga J., Ohtani H. and Igarashi K., **Denki Kagaku**, Vol. 49, No. 1 (1981), 19-21.
[15] "Thermodynamic Assessment of Fe-Tb and Fe-Dy Phase Diagrams and Prediction of Fe-Tb-Dy Phase Diagram", Landin S. and Ågren J., **Journal of Alloys and Compounds**, Vol. 207/208 (1994), 449-453.
[16] "Thermodynamic Investigation of the Rare-Earth Oxide Chlorides", Baev A.K. and Novikov G.I., **Russian Journal of Inorganic Chemistry**, Vol. 10 (1965), 1337-1341.
[17] "Electrowinning of Neodymium from a Molten Oxide-Fluoride Electrolyte", Dysinger D.K. and Murphy J.E., **Bureau of Mines - Report of Investigation**, RI 9504 (1994).
[18] Knacke O., Kubaschewski O. and Hesselmann K. (eds.), **Thermochemical Properties of Inorganic Substances**, Vol. 2, Springer-Verlag, 1991.
[19] "Enthalpy of Formation of Neodymium Dichloride and Thulium Dichloride", Morss L.R. and McCue M.C., **Inorganic Chemistry**, Vol. 14, No. 7 (1975), 1624-1627.
[20] "Methods of Estimating the Entropies of Solid Compounds", Latimer W.M., **Journal of the American Chemical Society**, Vol. 73 (1951), 1480.
[21] "Passivation of the Aluminium Cathode During Deposition of Aluminium from Aluminium Chloride-Sodium Chloride Melts", Bjørgum A., Sterten Å., Thonstad R., Tunold R. and Ødegård R., **Electrochimica Acta**, Vol. 29, No. 7 (1984), 975-977.

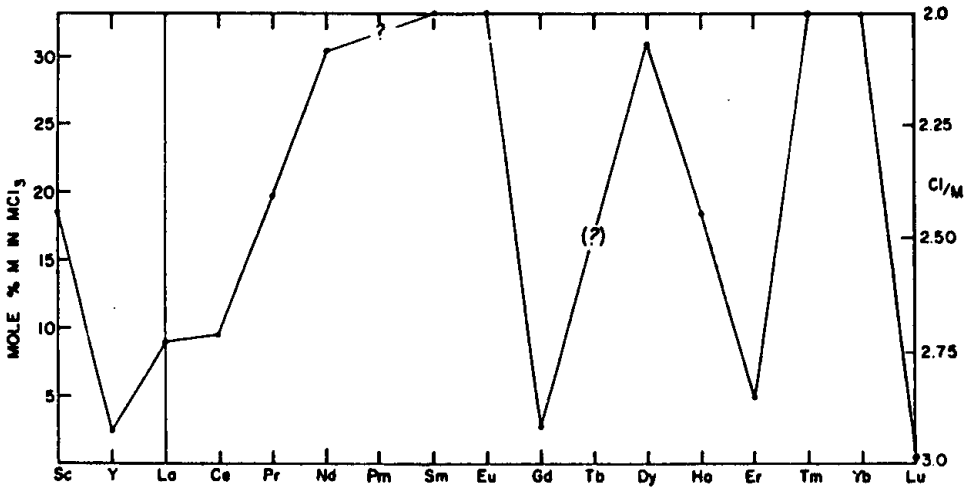

Figure 1. Composition of the molten chloride phase (as mol% metal and Cl/R) in equilibrium with the respective metal near 800°C. Values (?) of Cl/Pm and Cl/Tb are estimated. (Corbett [10])

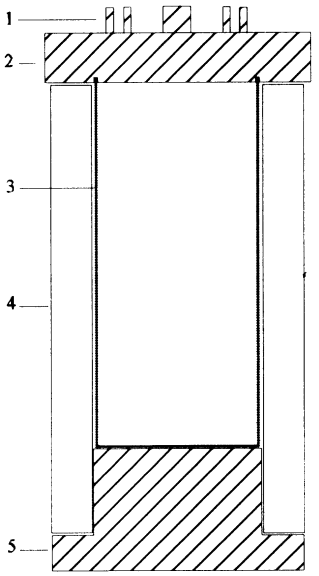

1. Mullite tubes 2. Alumina lid 3. Steel pot 4. Kanthal furnace 5. Alumina supporter

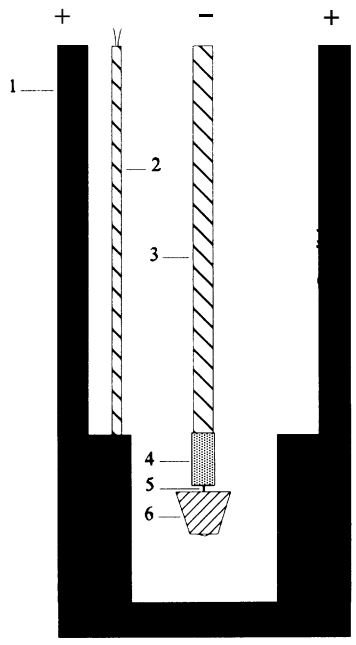

1. Anode, graphite container 2. Thermocouple protec-tion tube (Al_2O_3) 3. Cathodic lead protection tube (SiO_2) 4. Iron cathode 5. Tantalum wire 6. Al_2O_3 crucible

Figure 2. Left drawing: frame of the electrolytic cell. Right drawing: arrangement of the electrolytic cell.

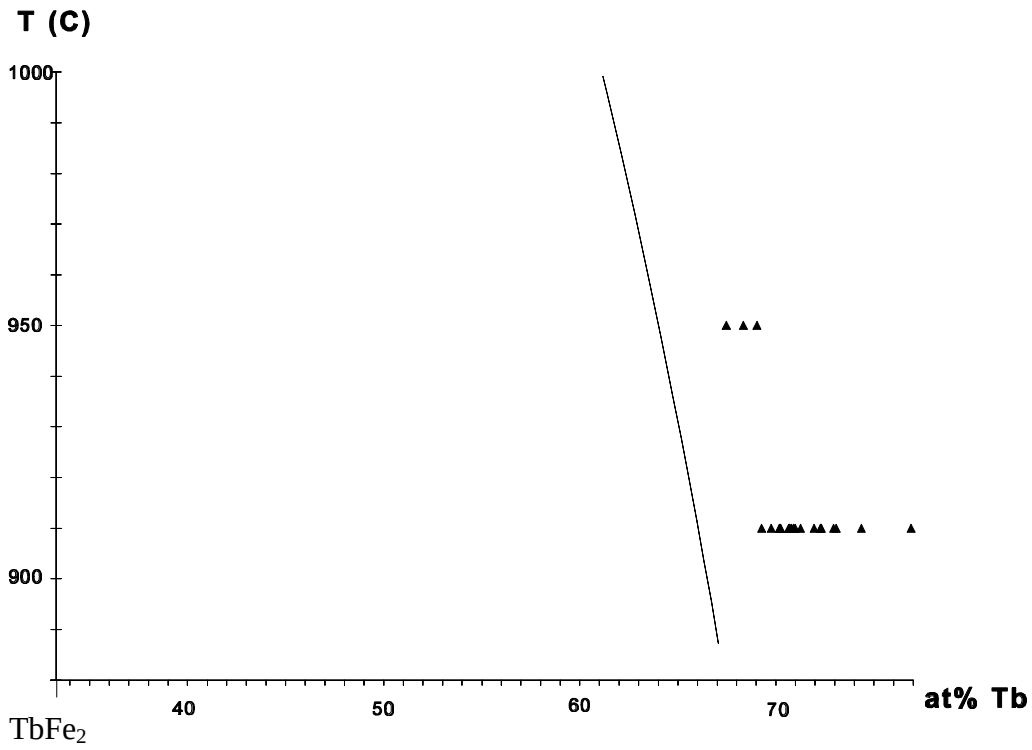

Figure 3. Composition (▲) of alloys from $TbCl_3$ electrolysis versus temperature in relation to the $TbFe_2$-liquidus line [15].

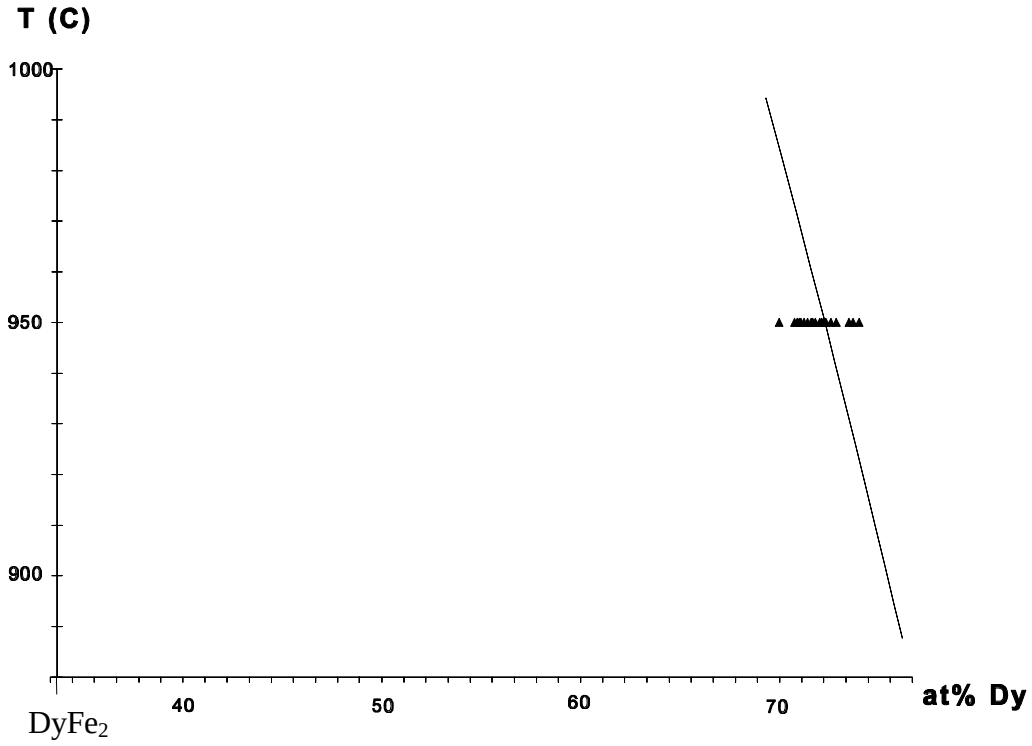

Figure 4. Composition (▲) of alloys from $DyCl_3$ electrolysis versus temperature in relation to the $DyFe_2$-liquidus line [15].

Figure 5. Light optical micrograph showing the microstructure of a former liquid film around the cathode (white upper area). White phase in liquid film is $DyFe_2$-crystals. Magnification 50x.

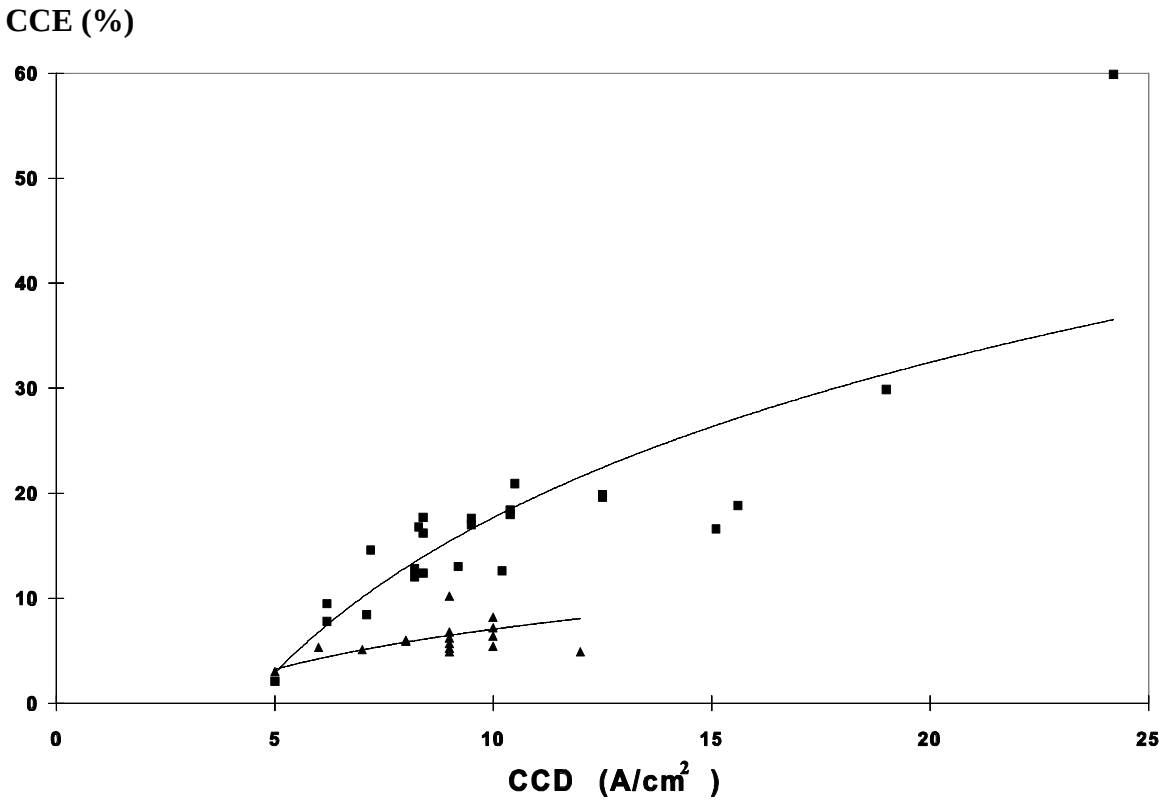

Figure 6. The relation between CCD and CCE. ■: $TbCl_3$ electrolysis. ▲: $DyCl_3$ electrolysis. Logarithmic lines have been adapted to the plotted data.

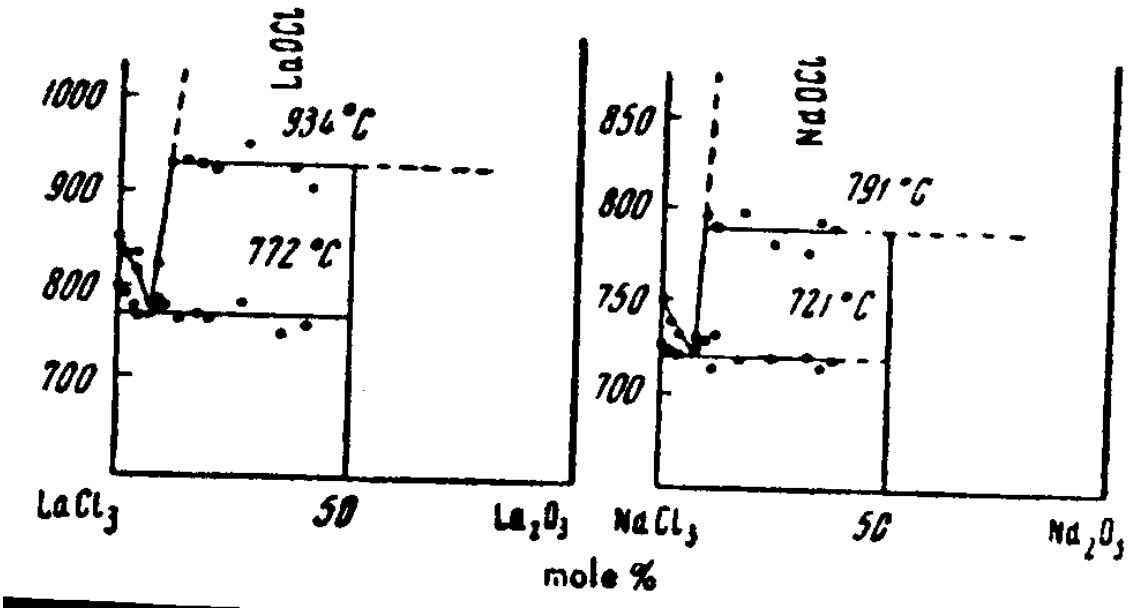

Figure 7. Phase diagram of $LaCl_3$-La_2O_3 (left) and $NdCl_3$-Nd_2O_3 (right) by Baev & Novikov [17].

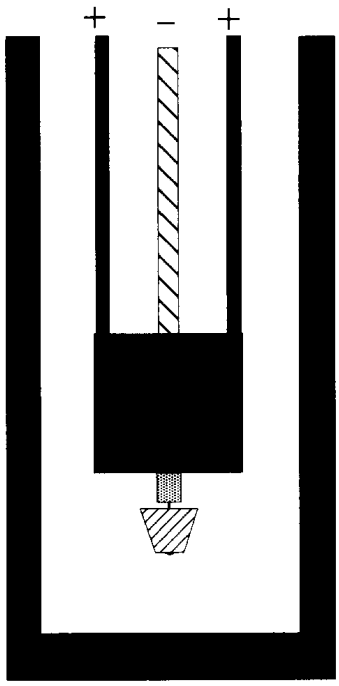

Figure 8. Cell arrangement used in the first two preliminary investigations.

Table 1. Experimental data and results of $TbCl_3$ electrolysis. (20/40/40 mol% $TbCl_3$/LiCl/LiF). Estimated final composition of $TbCl_3$=15 mol%.

cathode no:	T °C	I (A)	CCD_i/CCD_{av} (A/cm^2)	U (V)	t (min)	m_a (g)	CCE (%)
C1	910	69	8/8.2	3.6	40	13.3	12.8
C2	"	"	8/8.3	4.1	"	17.2	16.8
C3	950	"	8/8.2	4.1	"	12.7	12.0
C4	910	52	6/6.2	3.6	50	9.4	9.5
C5	"	86	10/10.4	4.9	30	17.5	18.0
C6	950	78	9/9.5	4.5	35	17.7	17.0
C7	910	"	9/9.5	4.6	"	18.1	17.6
C8	"	103	12/12.5	6.0	25	19.3	19.9
C9	"	60	7/7.1	2.5	45	8.5	8.4
C10	"	"	15/15.6	6.7	20	18.4	18.8
C11	"	43	5/5.0	2.6	60	2.0	2.1
C12	"	155	18/19.0	9.3	16	27.4	29.9
C13	950	86	10/10.4	4.9	30	18.0	18.4
C14	910	69	8/8.4	4.1	40	17.2	16.2
C15	"	"	8/8.4	4.2	"	12.8	12.4
C16	"	190	22/24.2	12.0	12	~50*	59.9*
C17	"	52	6/6.2	1.6	55	10.0	7.8
C18	"	69	8/8.4	2.7	40	18.4	17.7
C19	"	60	7/7.2	2.9	45	14.8	14.6
C20	"	78	9/9.1	4.5	30	4.7	5.5
C21	"	86	10/10.2	5.3	25	10.1	12.6
C22	"	103	12/12.5	6.5	24	18.3	19.6
C23	"	78	9/9.2	5.0	30	11.3	13.0
C24	"	86	10/10.5	5.4	"	20.4	20.9
C25	"	129	15/15.1	7.7	6	4.8	16.6

Table 2. Experimental data and results of $DyCl_3$ electrolysis. (20/40/40 mol% $DyCl_3$/LiCl/LiF).

* Crucible with alloy was not recovered from the electrolyte; m_a and CCE were estimated from the reduced volume of the cathode.

Estimated final composition of $DyCl_3$=18 mol%.

cathode no:	T °C	I (A)	CCD_i (A/cm^2)	U (V)	t (min)	m_a (g)	CCE (%)
C1	950	77.5	9	4.4	60	18.5	10.2
C2	"	86	10	5.0	50	12.1	7.2
C3	"	69	8	4.2	60	9.5	5.9
C4	"	77.5	9	4.5	40	8.3	6.8
C5	"	"	"	"	50	8.0	5.2
C6	"	"	"	"	"	9.5	6.2
C7	"	"	"	"	"	8.7	5.7
C8	"	86	10	5.0	16	3.5	6.4
C9	"	"	"	4.9	50	9.2	5.4
C10	"	69	8	4.1	60	9.7	6.0
C11	"	86	10	4.9	50	13.9	8.2
C12	"	60	7	3.9	70	8.5	5.1
C13	"	103	12	5.9	40	7.8	4.9
C14	"	52	6	3.6	74	7.9	5.3
C15	"	43	5	3.4	70	3.5	3.0
C16	"	77.5	9	4.5	50	7.4	4.9

Table 3. Equilibrium constants for oxidizing reactions of neodymium chloride at 900°C. Free energy data of solid compounds have been extrapolated up to 900°C.

Reaction:		K_{eq} (T=900°C, R=Nd)
$RCl_3(l) + ½O_2(g) = ROCl(s) + Cl_2(g)$	(3)	47
$RCl_3(l) + H_2O(g) = ROCl(s) + 2HCl(g)$	(4)	380
$RCl_2(s) + ½O_2(g) = ROCl(s) + ½Cl_2(g)$	(5)	$15 \cdot 10^{11}$
$RCl_2(s) + H_2O(g) = ROCl(s) + HCl(g) + ½H_2(g)$	(6)	$36 \cdot 10^{7}$